ASEAN Journal of Chemical Engineering 2023, Vol. 23, No. 1, 77 – 93

Spent Coffee Grounds Biochar Composite Phase Change Material Design Challenges in a Lab-Scale Solar Water Heater System for Thermal Energy Storage

Raphael Angelo Mondragon
Sasipa Boonyubol
Shuo Cheng
Jeffrey Scott Cross*
Department of Transdisciplinary Science and Engineering, School of Environment and Society, Tokyo Institute of Technology, 2-12-1 I4-19 Ookayama, Meguro-ku, Tokyo, 152-8550, Japan
*e-mail: cross.j.aa@m.titech.ac.jp

Submitted 12 December 2022 *Revised* 18 March 2023 *Accepted* 21 March 2023

Abstract. Thermal energy storage systems that use composite phase change materials (CPCM), such as paraffin wax and nonbiodegradable high-density polyethylene, are gaining attention in recent years due to the effort to resolve energy issues. There is a need to undertake research and development on how to prepare durable CPCMs from thermo-chemically treated biowastes, a renewable resource. Raw spent coffee grounds (SCG) have been experimented on previously, but more research needs to be conducted on CPCMs prepared from pyrolyzed SCG-biochar (SCGB) for use in a water tank. This research investigated a biodegradable CPCM made from SCGB and carnauba wax in a lab-scale solar water heater system. The carnauba wax loading of 60% was chosen due to the minimized thermal wax leakage from the PCM. Thermal characterization results revealed that the latent heat of SCGB CPCM is 88.47 J/g which was found to be competitive compared to other biodegradable CPCMs reported earlier. The results also show further potential for using SCGB and carnauba wax as a CPCM in a thermal energy storage system.

Keywords: Biochar, Phase Change Material, Spent Coffee Grounds, Carnauba Wax, Solar Water-Heater, Thermal Energy Storage

INTRODUCTION

As the threat of global climate change continues to grow, energy demands are projected to increase worldwide with rising ambient temperatures (Van Ruijven et al. 2019). Thermal energy storage is becoming a more important topic to conserve energy (Sharma et al. 2009). By improving thermal energy storage systems, energy utilization efficiency can be improved, and fossil fuel energy usage can be reduced.

Thermal energy storage systems typically work by storing energy in a solid or liquid medium that can be used later for heating or cooling (Sarbu and Sebarchievici, 2018). It can be accomplished through sensible heat storage, latent heat storage, or both (LibreTexts Engineering, 2021). Latent heat storage refers to phase change materials (PCMs) that store or release heat as the material changes phase (LibreTexts

DOI: 10.22146/ajche.80081

Engineering, 2021; Sarbu and Sebarchievici, 2018). Two typical PCMs are paraffin and salt hydrates (LibreTexts Engineering, 2021). However, they each have their shortcomings. Paraffin has low thermal conductivity, while salt hydrates melt incongruently (Kenisarin and Mahkamov, 2007; LibreTexts Engineering, 2021). Another problem with PCMs in general is thermal leakage (mass loss) that occurs during the phase change when heated above the wax melting temperature (Li et al. 2014). Even though encapsulation can help to solve this problem, it is somewhat costly. To address this problem, several studies (Ehid and Fleischer, 2012; Kaygusuz and Sari, 2007; Qu et al. 2019) have examined using supporting materials with porous structures such as non-biodegradable high-density polyethylene (HDPE) used to encapsulate paraffin (Kadohiro et al. 2021, 2020). Although these porous supporting materials could improve the performance of the PCM, the waste biomass is also a promising alternative due to its natural porous structure and environmental sustainability. Moreover, only a few research publications have addressed this issue using higher melting temperature natural waxes.

To increase environmental sustainability, this research aims to broaden the range of sustainable materials that can be used to support PCM. Carnauba wax (melting point: 82.8 °C) is a natural plant-based wax used to evaluate its effectiveness as a PCM. The supporting material to be tested in this research is spent coffee grounds (SCG) biochar. The SCG is the remaining solid residue after the coffee-making process. Since raw biomaterial is often discarded as waste, this research aims to broaden the usage of this waste biomass. The SCG was added as a scaffold or matrix to hold the wax and promote heat transfer more uniformly. Through the pyrolysis of these materials, bio-oil can also be produced as a by-product, which can potentially be used for biofuels or biochemicals (Yasser, 2022).

The utilization of raw SCG has previously been researched by Yoo et al. (2019) and Hu et al. (2021). The research done by Yoo et al. combined raw SCG with different natural waxes such as beeswax (melting point: 55.1 °C), palm wax (melting point: 60.6 °C), golden soy wax (melting point: 49-52 °C), and nature soy wax (melting point: 53.6 °C). The resulting composite PCM (CPCM) was form-stable and had excellent thermal properties with the highest latent heat value of 76.39 J/g. Furthermore, the research done by Hu et al. combined raw SCG with reduced graphene oxide (rGO) and polyethylene glycol (PEG). Combining raw SCG with rGO was able to increase the thermal conductivity and improve the adsorption of PEG to the SCG. The CPCMs also showed good reusability and excellent light-to-heat conversion. The biochar of raw SCG has yet to be used in the application of PCMs. Thus, this research hopes to address this knowledge gap and see how SCG-biochar (SCGB) performs.

Previous research studies investigating PCMs containing SCG and wax have not examined their thermal stability in hot water. While biochar made from other types of biomass, such water hyacinth (Das et al. 2020), rice husk (Jeon et al. 2019), pinecone (Wan et al. 2019), miscanthus straw (Atinafu et al. 2020), and almond shell, (Chen et al. 2018) has been experimented with, only thermal characterization has been done in almost all these studies. In the research conducted by Das et al. (2020) using water hyacinth, the CPCM was implemented in a solar dryer, but the working fluid or medium was hot air. Thus, how biochar based CPCMs would perform in a water environment is still

being determined. By testing the CPCM in a lab-scale solar water heater system, its potential for possible scaling-up can also be examined. The CPCM was also tested on how well it addresses the thermal leakage problem and how the thermal properties compared to other biodegradable CPCMs.

This research aim is to consider how the PCM materials' design and processing conditions impact its stability and thermal properties for use in a solar water heater system previously reported by Kadohiro et al. (2021). In the prior system, an HDPE/paraffin CPCM was used for heat storage in a hot/cold water tank. In this research, the biodegradable CPCM of carnauba wax and SCGB was studied to reveal the potential of this heat-treated biomass waste for energy storage applications. The applicability of this CPCM was also evaluated.

MATERIALS AND METHODS

Materials

The raw SCGs were obtained for free from the 7-Eleven convenience store in the Tokyo Institute of Technology's Ookayama campus, Meguro-ku, Tokyo, Japan. The powdered carnauba wax (Yamaki Sangyo Co., Ltd., Osaka, Japan, melting point: 82.8 °C) was used as the PCM. The raw SCGs were pyrolyzed into biochar and then mixed with the carnauba wax through a vacuum impregnation to form a SCGB CPCM. The Carnauba wax loading was varied in the range of 50% - 80% to find the optimum value with minimal leakage for this CPCM system.

Preparation

The preparation process of SCGB CPCM is illustrated in Figure 1. First, the raw SCGs were sieved to obtain a particle size of less than 1.7 mm. This particle size is based on previous studies (Das et al. 2020; Jeon et al. 2019) that used 2 mm as the particle size for their biochar samples. The raw biomaterial was turned into biochar through pyrolysis at 450 °C. This setting is based on the study done by Jeon et al. that also used biochar for latent heat storage biocomposites (Jeon et al. 2019). The ramp-up time starting from room temperature was about 15 minutes, and the holding time was 10 minutes. Nitrogen gas was used with a flow rate of 0.5 L/min. After pyrolysis, the biochar was dried in a hot air oven at 110 °C for 24 hours to reduce the water content present in the pores of the biochar and achieve a constant weight. The vacuum impregnation method was used to incorporate wax into the biochar pores. The powdered carnauba wax was first dry-mixed (Xu and Li, 2013) with the biochar then it was put in a vacuum oven (Yamato DP23, Yamato Scientific Co., Ltd., Tokyo, Japan) at 110 °C for 1 hour with a pressure of 0.1 kPa. The resulting CPCM was referred to as Carnauba:SCGB to indicate the mixture of carnauba wax and SCGB.

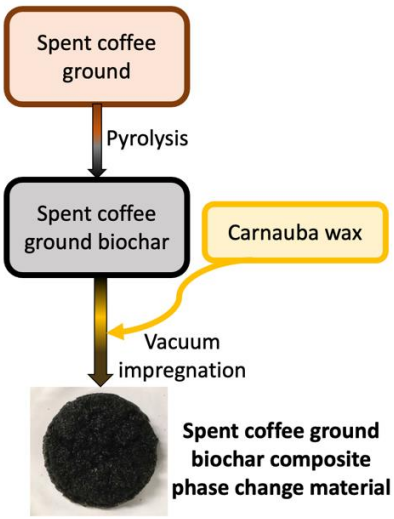

Fig. 1: The preparation process of SCGB CPCM.

A wax thermal leakage test was conducted to determine the appropriate wax loading of the CPCM. Biochar was mixed with carnauba wax in a vacuum oven then the mixture was put on filter paper and placed in a hot air oven at 110 °C for 30 minutes. Weight measurements of the sample before and after putting them in the oven show the amount of wax that has leaked out and was absorbed by the filter paper. The weight loss of the sample from the leakage test is calculated using Eq. (1) in which W_1 and W_2 are the weight of the sample before and after putting in the oven, respectively. This method of using filter paper to check for leakage was also used in several studies (Chen et al. 2018; Das et al. 2020; Hu et al. 2021; Jeon et al. 2019; Wan et al. 2019).

$$\text{Weight Loss } [\%] = \left(\frac{W_1 - W_2}{W_1}\right) \times 100 \quad (1)$$

Characterization Tests

Characterization tests were performed to determine the materials' composition and properties. The results showed what aspects of the materials were satisfactory based on the literature comparison and what needs improvement of thermal energy storage. A scanning electron microscope (VE-8800, Keyence, Osaka, Japan) was used to obtain morphological data of the biochar and CPCM samples. The samples were coated beforehand with gold using a magnetron sputter (MSP-1S, SHINKUU Device, Ibaraki, Japan) to increase the quality of the images. Fourier transform infrared spectroscopy (FT/IR-4600, JASCO, Tokyo, Japan) was used to determine the surface functional groups and chemical stability of the samples through the KBr pellet method. Laser flash analysis (NETZSCH LFA-457 MicroFlash, NETZSCH Japan K.K., Kanagawa, Japan) was used to determine the thermal conductivity of the samples. Samples were measured three times at room temperature with pyroceram as the reference sample. Preparation was done by Pt+C coating. Differential scanning calorimetry (Shimadzu DSC-60 Plus, SHIMADZU Corporation, Kyoto, Japan) determined the latent heat and phase change temperatures. The samples were measured from room temperature to 110 °C at a heating rate of 5 °C/min. Thermogravimetric analysis (TG-DTA2020SA-TK21, Bruker Japan Co., Ltd., Kanagawa, Japan) was conducted to determine the thermal stability of the samples. This analysis was conducted under argon flow (30 mL/min) from room temperature to 500 °C at a heating rate of 5 °C/min.

Experimental Design

Solar Water Heater System

The schematic diagram of the solar water heater system used in this experiment is shown in Figure 2. It was constructed and designed by Kadohiro et al. (2021).

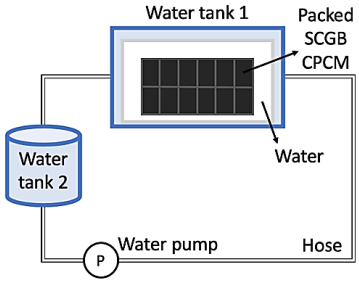

Fig. 2: The schematic diagram of solar water heater system constructed and designed by Kadohiro et al. (2021).

The system consists of two water tanks, a water pump, a flat aluminum heat pipe, and a halogen lamp (Ushio UL-PH-01, Ushio Lighting Inc., Tokyo, Japan). Water tank 1 is the heat storage media which contains both water and the CPCMs. Light from the halogen lamp heats the heat pipe that is connected to both the water tubes and water tank 1. The

water pump cycles the water between the heat pipe connected to water tank 1 and water tank 2. Light from the halogen lamp was used as a replacement for the actual sunlight.

Solar Water Heater System PCM in Daytime and Nighttime Operation

The daytime operation is focused on the system's efficiency in converting the light from the halogen lamp to thermal energy. The halogen lamp was set to 85 V and 40 W. The halogen lamp is placed 20 cm above the Fresnel lens. During daytime operation, the valves are closed off to reduce the heat loss in the water-cooling jacket. A fan is pointed toward the halogen lamp to prevent it from overheating.

Instead of heating the water in the heat storage media from room temperature to 95 °C, hot water was placed inside for time efficiency. The temperature in the water tank 1 was stabilized before beginning the daytime operation. The daytime operation took 4 hours and was performed at a temperature range of 70-95 °C.

Once the temperature of water reached 95 °C in the daytime operation mode, the nighttime operation mode began. The halogen lamp was turned off, and water tank 2 was filled with cold water. The valves were opened, and the pump was turned on to allow the water to flow through the system. The pump operated at a flow rate of 0.16-0.20 L/min.

The theoretical temperature of water tank 1 is calculated using Eq. (2) for daytime operation mode and Eq. (3) for nighttime operation mode, respectively. These are the same calculations used in Kadohiro's study (Kadohiro et al. 2021). The derivation of each equation was explained in more detail in Kadohiro's study.

$$T_{w1} = \left(\frac{\dot{Q}_h - \dot{Q}_{w1loss} - \dot{Q}_{lrc} - \dot{Q}_{wj}}{m_w c_{pw} + m_{pcm} c_{ppcm}}\right) t + T_{i1} \quad (2)$$

Here, T_{w1} is the temperature in water tank 1, $\dot{Q}_h$ is the concentrated solar radiation on the target, $\dot{Q}_{w1loss}$ is the convective heat loss from water tank 1, $\dot{Q}_{lrc}$ is the convection and radiation loss from the concentrated part, $\dot{Q}_{wj}$ is the thermal energy stored in the water-cooling jacket, m_w is the mass of water in water tank 1, c_{pw} is the specific heat of water, m_{pcm} is the mass of CPCM in water tank 1, c_{ppcm} is the specific heat of CPCM, t is time, and T_{i1} is the initial temperature in water tank 1.

$$T_{w1} = T_{i1}\, exp\left(-\frac{\beta}{(m_w c_{pw} + m_{pcm} c_{ppcm})} t\right) + \frac{\alpha}{\beta}\left(exp\left(-\frac{\beta}{(m_w c_{pw} + m_{pcm} c_{ppcm})} t\right) - 1\right) \quad (3)$$

The expressions of α and β are shown below in Eq. (4) and (5), respectively.

$$\alpha = \dot{Q}_{w1loss} - \frac{2\dot{m} c_{pw} T_{in}}{1 + 2\dot{m} c_{pw} R} \quad (4)$$

$$\beta = \frac{2\dot{m} c_{pw}}{1 + 2\dot{m} c_{pw} R} \quad (5)$$

Here, $\dot{m}$ is the mass flow rate of water, T_{in} is the water temperature at the inlet of the water-cooling jacket, and R is the total thermal resistance.

RESULTS AND DISCUSSION

SEM Analysis

The morphology of SCGB and Carnauba: SCGB CPCM at different wax loading of 60, 70, and 80% can be seen in Figure 3. It can be observed in Figure 3(a) that pores are present

in the structure of the SCGB, which suggests the potential for wax to be filled in and stored in these pores. The texture differentiates the biochar from the wax in the Carnauba/SCGB image (Figure 3(b)). The rough texture of biochar and the smooth surface texture of carnauba wax are present. From the Carnauba/SCGB image, wax can be seen which confirms that it can be adsorbed within the pores of SCGB. However, the empty pores or voids can still be observed. This could mean that the vacuum impregnation method might not be able to incorporate the wax into the pores fully or the amount of wax was not enough. This could also mean that the CPCM can take a higher wax loading.

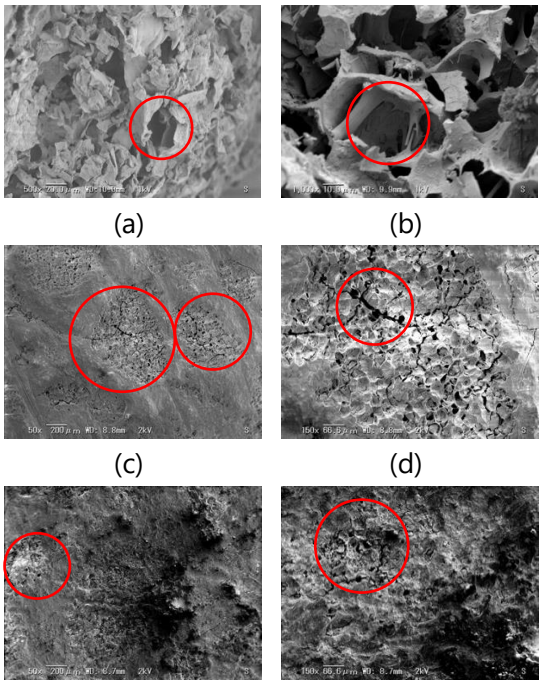

Fig. 3: SEM images of (a) SCGB at 500x; (b) 60:40 Carnauba/SCGB at 1000x; (c) 70:30 Carnauba/SCGB at 50x and (d) 150x; (e) 80:20 Carnauba/SCGB at 50x and (f) 150x with pores encircled.

As a result, the wax loading was increased to 70%. In Figure 3(c) and Figure 3(d), it can be observed that the surface of the sample looks mostly smooth. Therefore, the sample has adsorbed a higher wax content due to the increased wax loading. Most of the surface is covered with wax. However, the regions of empty pores are still present. This shows that there are still spaces that carnauba wax can fill in. Therefore, the wax loading was increased again to 80%, in which the morphology can be seen in Figure 3(e) and Figure 3(f). The surface is mostly covered with wax with smaller regions of pores that appear empty without wax filling. The change in morphology could be observed by SEM image alone. However, the optimal amount of wax loading could not be fully justified. Therefore, the leakage test was carried out.

Leakage Test

The leakage test was performed to measure the weight loss before and after the vacuum impregnation to determine the optimal wax loading. Figure 4 illustrates the CPCMs with different wax weight compositions after the leakage test.

For the CPCM with 80% wax loading shown in Figure 4(a), it can be clearly observed that the wax is overflowing, indicating the excess amount of wax. This could also make the sample unstable since the SCGB can flow out. The weight loss results are summarized in Table 1.

Although the sample with 70% wax loading was form-stable, the weight loss of the sample with 60% wax loading was half that with 70%. The weight loss difference between 50% and 60% of wax loading was not as much as the weight loss difference between 60% and 70%. Furthermore, it could be seen in the sample with 50% wax loading in Figure 4(d) that some pieces of biochar broke off, indicating the sample's brittleness. Thus, Carnauba:SCGB at 60:40 was chosen to address the leakage problem while still

having a large amount of wax for storing and releasing heat. SCGB could hold wax and prevent most of it from leaking out because of the capillary and surface tension forces acting on the wax as it adsorbs to the biochar. This phenomenon was also observed in research with porous biochar (Atinafu et al. 2020; Chen et al. 2018; Das et al. 2020; Hu et al. 2021; Wan et al. 2019).

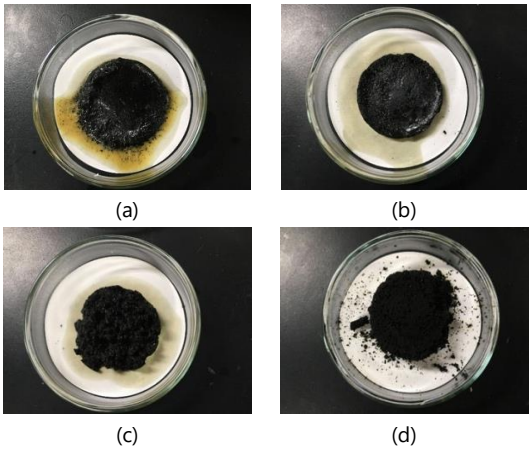

Fig. 4: Leakage test for Carnauba/SCGB CPCM with different weight compositions: Carnauba: SCGB = (a) 80:20; (b) 70:30 (c) 60:40 (d) 50:50

The differences in weight loss among the samples could be attributed to the wax loading. The samples may have already exceeded the adsorption capacity of the SCGB. Thus, with increasing amounts of wax being put in the biochar, there would also be increasing amounts of wax overflowing from the CPCM and leaking into the filter paper. Although it was shown in the SEM analysis that there were still unfilled pores, these types of pores may not be ideal for wax to adsorb to. When measured by BET, the SCGB had a relatively low surface area, indicating that biochar optimization could have resulted in greater surface area and higher wax loading.

Table 1. Leakage test results for different weight compositions of Carnauba:SCGB CPCM

Weight Composition	Wax loading (%)	Weight Loss (%)
80:20	80	6.45
70:30	70	6.12
60:40	60	3.76
50:50	50	2.24

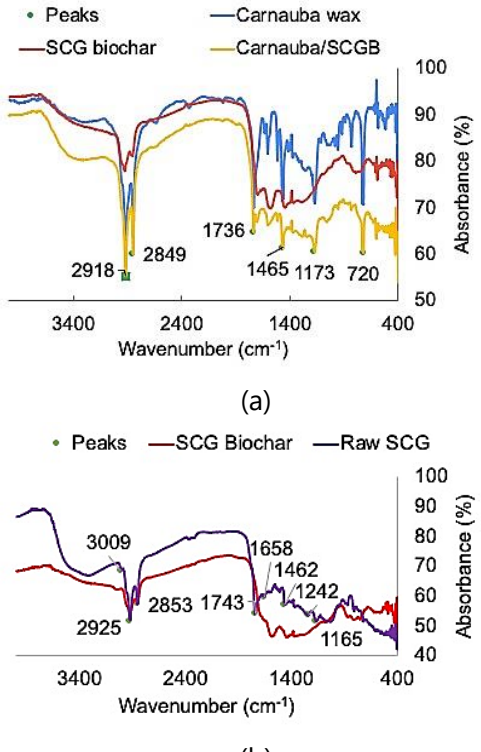

Fig. 5: (a) FTIR results of (blue) carnauba wax, (red) SCGB, and (yellow) Carnauba/ SCGB; (b) FTIR results comparing (red) SCGB, and (purple) raw SCG

FTIR Spectroscopy Analysis

Through FTIR spectroscopy analysis, the following data found in Figure 5 were obtained. In Figure 5(a), from 3000 cm^{-1} to 2000 cm^{-1}, two peaks were observed at 2918 cm^{-1} and 2849 cm^{-1}. These peaks can be identified as the C-H stretching vibration, known to be present in the coffee samples

(Ballesteros et al. 2014; Nguyen et al. 2022). From 2000 cm^{-1} to 1000 cm^{-1}, the peaks found at 1743 cm^{-1} and 1736 cm^{-1} are attributed to the C=O stretching of the carbonyl group (Yoo et al. 2019). The peak at 1658 cm^{-1} found in raw SCG is attributed to the bending vibration of OH- (Krishna Mohan et al. 2019). The large peaks found at 1465 cm^{-1} in carnauba wax and 1462 cm^{-1} in raw SCG are attributed to the C-H bending (Muscat et al. 2014). The peaks in carnauba wax at 1173 cm^{-1} and in raw SCG at 1165 cm^{-1} are attributed to C-O stretching (Muscat et al. 2014). Finally, from 1000 cm^{-1} to 400 cm^{-1}, the peak at 720 cm^{-1} refers to methylene (CH_2) (Robertson et al. 2020). It can be seen in the graph that the peaks found in carnauba wax and in SCGB were also found in Carnauba/SCGB. Since no new peaks were observed in Carnauba/SCGB, no chemical reactions occurred between the PCM and its supporting material. This result implies that the carnauba wax can coat the surface and fill the packed SCGB pores without chemical reactions.

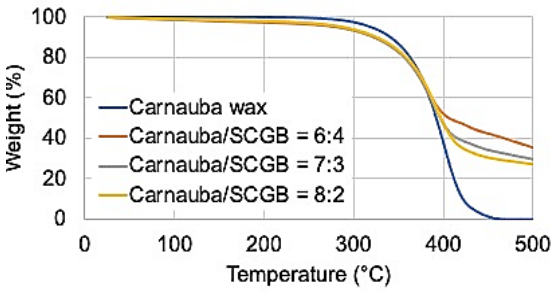

Fig. 6: Thermogravimetric analysis results of carnauba wax (blue), Carnauba:SCGB at 60:40 (orange), 70:30 (gray), and 80:20 (yellow)

Additionally, comparing raw SCG with SCGB in Figure 5(b), the two peaks at 2918 cm^{-1} and 2849 cm^{-1} were present in both samples. Outside these two peaks, the functional groups start to differ, especially from 1800 cm^{-1} onwards. The difference in thermal performance could also be attributed to the different functional groups between the two materials resulting from the structural change after pyrolysis.

Thermal Properties of SCG/Carnauba Wax

Thermogravimetric Analysis

Figure 6 shows the thermogravimetric analysis (TGA) results for carnauba wax and Carnauba/SCGB CPCM at different weight compositions.

Figure 6 shows that the weight loss was a linear process that is proportional to the temperature for the CPCM. From 0 °C to 193 °C, the weight of carnauba wax was constant. From 193 °C onwards, the wax starts to lose weight, which could mean that the wax starts to evaporate. In a previous study performed by Craig et al. (Craig et al. 1971), where TGA was also conducted on carnauba wax at a heating rate of 15 °C/min, weight loss was observed at higher temperatures from 246 °C. The weight loss from the CPCM samples happened earlier at approximately 100 °C, indicating a possibility that moisture was trapped in the samples which started to evaporate. Thus, it is concluded that carnauba wax is stable until a higher range at approximately 240 °C at which it starts to evaporate. From 240 °C to 450 °C the weight loss is attributed to the evaporation of carnauba wax. For the CPCM samples, it can be seen that there is still some weight loss that occurs after the evaporation of carnauba wax, which is the formation of biochar. Since the supporting material is biochar, it was already heated to 450 °C during pyrolysis. Thus, it is unlikely to degrade further at temperatures of less than 450 °C. Therefore, these TGA results show great stability of Carnauba/SCGB CPCM as

the operating temperature in a solar hot water storage system is less than 100 °C.

DSC and Laser Flash Analysis

Thermal conductivity of the samples was measured through laser flash analysis, while phase change temperatures and latent heat were evaluated using DSC analysis. The results are shown in Figure 7. The summary of the developments compared with Kadohiro's paraffin:HDPE CPCM is listed in Table 2. Based on the curves and the fact that only one peak is observed, it indicates that varying amount of carnauba wax affect the difference in the curves. Comparing the latent heat values, the SCGB latent heat values were significantly lower compared to that of carnauba wax alone. This is due to the density of the samples as the ones with higher wax loading can achieve a closer latent heat value to that of pure carnauba wax. It can be observed that with higher wax weight ratio, more heat can be stored by the CPCM. Moreover, with higher wax loading, the wax could occupy more empty pores, which would increase the latent heat values. As expected, the sample with the wax loading of 80% has the highest latent heat value as shown in Table 2.

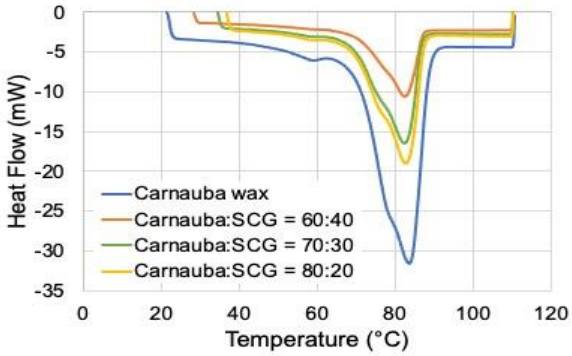

Fig. 7: DSC results of carnauba wax (blue), Carnauba:SCGB at 60:40 (orange), 70:30 (green), and 80:20 (yellow)

As for the thermal conductivity, the samples of Carnauba:SCGB significantly decreased compared to that of carnauba wax alone. This result is attributed to the lower density and porosity. While density is proportional to thermal conductivity, even if the CPCM managed to reach the maximum wax loading, the thermal conductivity still does not seem enough to reach a competitive value. For the CPCM to achieve higher thermal conductivity, higher density is needed. The samples' porosity then seems to be the other reason for the low thermal conductivity values. From Figure 3(c) and Figure 3(e), it could be seen that although the CPCM was able to take a higher wax loading,

Table 2. CPCM non-biochar vs biochar thermal conductivity and latent heat comparison with Kadohiro's system (Kadohiro et al 2021)

Sample	Melting Temperature [°C]	Latent Heat (melting/ freezing) [J/g]	Density [g/cm^3]	Thermal Conductivity [W/(m*K)]
Carnauba wax	70.79	165.69 / 167.02	0.833	1.102
Carnauba:SCGB = 60:40	72.82	88.47 / 93.73	0.465	0.109
Carnauba:SCGB = 70:30	70.72	115.29 / 117.47	0.581	0.119
Carnauba:SCGB = 80:20	71.02	123.93 / 122.50	0.613	0.168
Paraffin:HDPE = 80:20, EG 4.6wt% (Kadohiro et al., 2021)	59.77	145.5 / 155.0	0.952	0.508

there were still pores present that were not filled with wax. While empty pores could be seen on the surface, there may also be pores inside the sample filled with air. These air pockets in the pores can be a reason for the lower thermal conductivity.

Comparing the thermal properties, with the same wax loading, the latent heat value is quite close to that of the paraffin:HDPE. However, the thermal conductivity value is much lower. As discussed earlier, this could be attributed to the porosity of the sample. The paraffin:HDPE sample encounters a different problem since HDPE is non-porous. Density is also another factor. The non-porous nature of HDPE would be able to use the extra space to hold more wax compared to SCGB with empty pores. Furthermore, the paraffin:HDPE sample is mixed with expanded graphite (EG), a thermally conductive filler. While paraffin:HDPE may still be superior to Carnauba:SCGB CPCM in terms of thermal properties, it is important to note that carnauba wax and SCGB are made from biodegradable materials, which makes the CPCM environmentally friendly. The supporting material, SCG, is also often just thrown away, making the CPCM relatively inexpensive to fabricate.

Comparison with Literature

Table 3 compares the present study's thermal conductivity and latent heat values with those found in literature. The supporting materials from the chosen previous studies are also biodegradable and porous, which makes a good comparison to this work. The present study has proven to be very competitive in terms of latent heat (88.47 J/g) when compared to other studies. However, in terms of thermal conductivity, the value of the present study is still lower. Moreover, comparing these different studies to the paraffin:HDPE sample (0.508 W/(m·K)), shown in Table 2, it seems that using porous materials would generally result in a lower thermal conductivity value. Compared to studies that used raw SCG (Hu et al. 2021; Yoo et al. 2019), this study seems to have a large advantage regarding latent heat. The PCM's thermal properties may be a factor, but it is also possible that turning the raw biomaterial into biochar may make it more suitable for wax loading. The study done by Hu et al.

Table 3. Comparison of thermal analysis results of CPCM with previous studies

PCM	Supporting Material	Thermal Conductivity [W/(m*K)]	Latent heat [J/g]	References
Beeswax	SCG	-	50.77	Yoo et al. 2019
Palmwax	SCG		76.39	
Golden Soywax	SCG		21.05	
Nature Soywax	SCG		19.43	
PEG	SCGs@RGO	0.312	81.9	Hu et al. 2021
Paraffin wax	Water Hyacinth biochar	0.283	179.4	Das et al. 2020
PEG	Pinecone biochar	0.3926	84.74	Wan et al. 2019
PEG	Almond shell biochar	0.402	82.73	Chen et al. 2018
Carnauba wax	**SCGB**	**0.109**	**88.47**	**This study**

Table 4. Comparison between PCM non-biochar and biochar systems

	Kadohiro's system (Kadohiro et al., 2021)	**Al-Kayiem's system (Al-Kayiem and Lin, 2014)**	**Wu's system (Wu et al., 2018)**	**This study**
Supporting material	HDPE	None	None	SCGB
PCM	Paraffin wax	Paraffin wax	48#Paraffin wax	Carnauba wax
Wax loading [%]	80	100	100	60
Melting / Freezing Peak Temperature [°C]	69.9 / 62.8	60.5 / 58.7	48-50 °C (phase change temperature)	72.82 / 73.87
Operating Temperature [°C]	70-90	30-70	47-55	70-95
Latent heat (Melting/Freezing) [J/g]	145.5 / 155.0	166.7	234	88.47 / 93.73
Thermal conductivity	0.508 W/(m·K)	0.172 W/(m·°C)	-	0.109 W/(m·K)
Density [g/cm^3]	0.952	0.912	0.9086	0.465
Thermal additives	Expanded graphite at 4.6 wt%	None	None	None

(Hu et al. 2021) has a much higher thermal conductivity value, but it is also important to note that rGO is thermally conductive.

Solar Water Heater Data

In discussing solar water heater systems, only a few studies have examined incorporating PCMs within a system. Aside from Kadohiro et al. (2021) system, both Al-Kayiem et al. (Al-Kayiem and Lin, 2014) and Wu et al. (Wu et al. 2018) have also used paraffin wax as the PCM. The differences between these non-biochar systems and the one used in this study are listed in Table 4.

While these studies provide comparison by showing what standard materials are used in solar water heater systems, the most relevant non-biochar system to which this study can be compared is Kadohiro's system. Since this study also used Kadohiro's system to test the CPCM, the operating temperature is similar. The difference is the supporting material and PCM as shown in Table 4. It is important to note that for both Al-Kayiem's and Wu's systems, no supporting material was used and lower temperature was operated.

Daytime and Nighttime Operation Results

Through mathematical modeling, a thermal simulation program was written by Kadohiro et al. (2021) to simulate the performance and temperature of the system with PCMs, illustrated in Figure 8. Figure 8(a) shows the daytime operation results, while Figure 8(b) shows the nighttime operation results.

The Tw1_Theory (blue line) is the theoretical temperature of the water tank 1 in which Eq. (2) and Eq. (3) were used for the calculation of Tw1_Theory in Figure 8(a) and Figure 8(b), respectively. The

Tw1_Measurement (red dotted line) is given by the experimental temperature of water tank 1 from the measurement data.

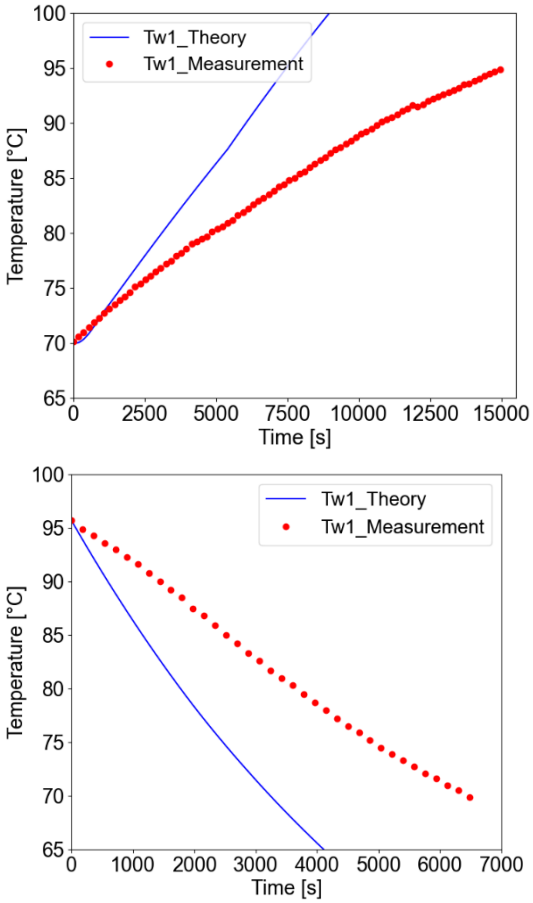

Fig. 8: Comparing (blue) theoretical temperature of water tank 1 (Tw1_Theory) with (red) experimental temperature of water tank 1 (Tw1_Measurement) for (a) daytime operation, and (b) nighttime operation

The experimental result is far from the theoretical result for the daytime operation results. The experimental result has a much shallower slope indicating the slow temperature increase in the system. These results could be attributed to two factors, one of which was also noted in Kadohiro's study. The first factor is related to the temperature gradient within the PCMs. Since the heat was transferred through the heat pipes, this would cause the PCMs near the heat pipes melt first compared to the ones located further away. This non-simultaneous melting would result in a slower temperature increase than the theoretical calculation. This may make the PCMs take longer time to melt entirely. This would also be the reason why the theoretical line has a faster increase in temperature since this issue could not be factored into the mathematical modeling accurately. Another factor is the effect of the wet environment on the PCMs. After repeated use of the PCMs, some SCGB particles would eventually break off and float to the top of the water tank. When this happens and wax reaches the surface of the water, the difference in temperature between the air above the water and the water itself might cause the wax to solidify. This would also mean that the PCMs would take longer to melt. As a result, the system could not take full advantage of the PCM's thermal properties. To address this problem, the CPCM density and thermal conductivity should also be optimized for use with hot water in future work.

The nighttime operation results show that the experimental results also have a shallower slope indicating a longer freezing time. The cause for this slow freezing time could also be attributed to the same factors listed in the daytime operation results. Although PCMs should have a constant temperature between the melting and freezing points, none is observed in the graph. This is due to the use of water in water tank 1. With water in the heat storage system, the PCMs could undergo phase change. Since water is still in liquid, it would only absorb or release sensible heat as it does not change phase throughout the temperature range. Conversely, the CPCMs absorb or release latent heat during phase change and absorb or release sensible heat otherwise. Thus, the

graph combines both the absorption/release of sensible heat and latent heat. A positive effect of longer freezing time is that heat can be stored longer in the system at night. If people were to install this system on their rooftops, they would have sufficient time to use all the heat stored during the daytime making this a favorable aspect of this experiment.

The wax leakage problem could be addressed by using a superhydrophobic coating similar to what was done by Yang et al. (Yang et al. 2020). With a superhydrophobic coating, water would not seep in which could prevent leakage and optimize the CPCM for use in water. This would preserve the thermal properties of the CPCM in humid or wet environments. For a fully biodegradable system, there are several biodegradable superhydrophobic coatings are being researched on such as the works by Dong et al. (Dong et al. 2019), Cheng et al. (Cheng et al. 2017), Milionis et al. (Milionis et al. 2014) and Huang et al. (Huang et al. 2017). However, these biodegradable superhydrophobic coatings have yet to be tested on PCMs. Therefore, it is also possible to explore these coatings' interaction with PCMs and optimize it for usage in a solar water heating system. Potentially, wax leakage could also be reduced by using smaller SCG particles with higher surface area to form a denser structure with lower porosity.

Thermally conductive fillers such as expanded graphite might be needed to improve thermal conductivity. However, one problem noted is the aggregation of the filler particles during the melting process. To counteract this, other studies have tried turning these fillers into a 3D skeleton (Li et al. 2020; Wei et al. 2021; Wu et al. 2020) using rGO, three-dimensional graphene, or graphene aerogels. By turning the fillers into a 3D porous structure, the leakage problem would also be addressed. The structure would also give the CPCM additional mechanical strength which is important if the packaging is considered in the design process. With both solutions, the main challenge is finding a biodegradable material to fit the sustainability theme.

In this research, the PCM wax thermal leakage test was selected as the key design parameter by which the wax to SCGB ratio was fixed. By selecting a 60% wax loading, which was the ratio with the least amount of leakage, the thermal properties were lower than with higher wax loadings. However, the PCMs were used in water ranging from room temperature to 95 °C. The thermal leakage test conducted in air and the PCM used in the hot water tank did show some similarities e.g., wax leaked out in air and hot water.

For future work and in the pursuit of achieving durable and higher thermal conductivity PCMs, the leakage test conducted should be in the same environment as the system in which it will be used. It is often the case that leakage tests are conducted in air (Chen et al. 2018, p.; Das et al. 2020; Jeon et al. 2019; Kadohiro et al. 2021; Wan et al. 2019). However, suppose biodegradable CPCMs will be used together in water at various temperatures for a more effective heat storage unit. In that case, the key design parameter should consider the PCM operating environment. This way, the most suitable wax loading and thermal stability would contribute to better thermal properties.

In addition, the higher surface area of SCGB with smaller particle sizes and lower porosity with higher wax loadings should also be further investigated. In a study by Tan et al. (Tan et al. 2018), increasing the pyrolysis

temperature resulted in a higher surface area in the biochar. Biochar prepared under carbon dioxide instead of nitrogen resulted in more developed pore structures. These results suggest the potential for higher wax loading. Furthermore, the particle size used in the current study was less than 1.7 mm, based on previous studies (Das et al. 2020; Jeon et al. 2019). With lower particle sizes, the biochar surface area may increase. Thus, by optimizing the biochar, wax loading and thermal properties could be improved, and the number of empty pores would decrease.

CONCLUSIONS

In this study, a lab-scale biodegradable form-stabilized CPCM was made from SCGB and carnauba wax. Using a wax loading of 60%, the thermal wax leakage problem in the air was minimized. Although the CPCM had a thermal conductivity of 0.109 W/(m*K), the latent heat value of 88.47 J/g was very competitive compared to other biodegradable CPCMs. Furthermore, using SCGB as the supporting material yielded higher latent heat values than studies that used raw SCG, which indicates the use of biochar as an advantage. The CPCM was also found to be stable up to 240 °C which shows great stability to keep warm water. Implementing the CPCM in the system, identified how the biodegradable CPCM can be optimized further to be successfully used for thermal energy storage. Further improvements are still required to increase the thermal conductivity and optimize the wax leakage problem in the hot water system. Thus, this study shows the potential of preparing biodegradable Carnauba:SCGB CPCMs which are environmentally sustainable and durable via further process optimization.

ACKNOWLEDGEMENTS

The authors thank the Open Research Facilities for Life Science and Technology, Tokyo Institute of Technology, for DSC analysis (for technical assistance). The authors would also like to thank Professor Katsumi Yoshida and Assistant Professor Anna Gubarevich of the Laboratory for Zero-Carbon Energy, Tokyo Institute of Technology, for Laser flash analysis and Thermogravimetric analysis measurements. The authors would also like to thank Professor Toshiyuki Ikoma and Assistant Professor Yasuhiro Nakagawa of Ikoma Laboratory for their assistance in FT-IR spectroscopy results. The authors are also grateful for the raw SCGs provided by the 7-Eleven convenience store (Tokyo Institute of Technology, Ookayama campus, Tokyo, Japan).

REFERENCES

Al-Kayiem, H.H., and Lin, S.C., 2014. "Performance evaluation of a solar water heater integrated with a PCM nanocomposite TES at various inclinations." *Sol. Energy, 109*, 82–92.

Atinafu, D.G., Chang, S.J., Kim, K.-H., and Kim, S., 2020. "Tuning surface functionality of standard biochars and the resulting uplift capacity of loading/energy storage for organic phase change materials." *Chem. Eng., J. 394*, 125049.

Ballesteros, L.F., Teixeira, J.A., and Mussatto, S.I., 2014. "Chemical, functional, and structural properties of spent coffee grounds and coffee silverskin." *Food Bioprocess Technol., 7*, 3493–3503.

Chen, Y., Cui, Z., Ding, H., Wan, Y., Tang, Z., and Gao, J., 2018. "Cost-effective biochar

produced from agricultural residues and its application for preparation of high performance form-stable phase change material via simple method." *Int. J. Mol. Sci., 19*, 3055.

Cheng, Q.-Y., An, X.-P., Li, Y.-D., Huang, C.-L., and Zeng, J.-B., 2017. "Sustainable and biodegradable superhydrophobic coating from epoxidized soybean oil and ZnO nanoparticles on cellulosic substrates for efficient oil/water separation." *ACS Sustain. Chem. Eng., 5*, 11440–11450.

Craig, R.G., Powers, J.M., and Peyton, F.A., 1971. "Thermogravimetric analysis of waxes." *J. Dent. Res., 50*, 450–454.

Das, D., Bordoloi, U., Muigai, H.H., and Kalita, P., 2020. "A novel form stable PCM based bio composite material for solar thermal energy storage applications." *J. Energy Storage, 30*, 101403.

Dong, X., Gao, S., Huang, J., Li, S., Zhu, T., Cheng, Y., Zhao, Y., Chen, Z., and Lai, Y., 2019. "A self-roughened and biodegradable superhydrophobic coating with UV shielding, solar-induced self-healing and versatile oil–water separation ability." *J. Mater. Chem. A, 7*, 2122–2128.

Ehid, R., and Fleischer, A.S., 2012. "Development and characterization of paraffin-based shape stabilized energy storage materials." *Energy Convers. Manag., 53*, 84–91.

Hu, X., Huang, H., Hu, Y., Lu, X., and Qin, Y., 2021. "Novel bio-based composite phase change materials with reduced graphene oxide-functionalized spent coffee grounds for efficient solar-to-thermal energy storage." *Sol. Energy Mater. Sol. Cells, 219*, 110790.

Huang, J., Wang, S., and Lyu, S., 2017. "Facile Preparation of a robust and durable superhydrophobic coating using biodegradable lignin-coated cellulose nanocrystal particles." *Materials, 10*, 1080.

Jeon, J., Park, J.H., Wi, S., Yang, S., Ok, Y.S., and Kim, S., 2019. "Characterization of biocomposite using coconut oil impregnated biochar as latent heat storage insulation." *Chemosphere, 236*, 124269.

Kadohiro, Y., Cheng, S., and Cross, J.S., 2021. "Solar thermoelectric lab-scale system with sensible/latent heat storage for reversible power generation and warm water heating." *J. Energy Storage, 44*, 103278.

Kadohiro, Y., Cheng, S., and Cross, J.S., 2020. "All-Day Energy Harvesting Power System Utilizing a Thermoelectric Generator with Water-Based Heat Storage." *Sustainability, 12*, 3659.

Kaygusuz, K., and Sari, A., 2007. "High density polyethylene/paraffin composites as form-stable phase change material for thermal energy storage." *Energy Sources Part A, 29*, 261–270.

Kenisarin, M., and Mahkamov, K., 2007. "Solar energy storage using phase change materials." *Renew. Sustain. Energy Rev., 11*, 1913–1965.

Krishna Mohan, G., Naga Babu, A., Kalpana, K., and Ravindhranath, K., 2019. "Removal of chromium (VI) from water using adsorbent derived from spent coffee grounds." *Int. J. Environ. Sci. Technol., 16*, 101–112.

Li, H., Chen, H., Li, X., and Sanjayan, J.G., 2014. "Development of thermal energy storage composites and prevention of PCM leakage." *Appl. Energy, 135*, 225–233.

Li, W.H., Lai-Iskandar, S., Tan, D., Simonini, L.,

Dudon, J.-P., Leong, F.N., Tay, R.Y., Tsang, S.H., Joshi, S.C., and Teo, E.H.T., 2020. "Thermal conductivity enhancement and shape stabilization of phase-change materials using three-dimensional graphene and graphene powder." *Energy Fuels, 34*, 2435–2444.

LibreTexts Engineering, 2021. 8.6: Applications of Phase Change Materials for Sustainable Energy — eng.libretexts.org [WWW Document]. URL

Milionis, A., Ruffilli, R., and Bayer, I.S., 2014. "Superhydrophobic nanocomposites from biodegradable thermoplastic starch composites (Mater-Bi®), hydrophobic nano-silica and lycopodium spores." *Rsc Adv., 4*, 34395–34404.

Muscat, D., Tobin, M.J., Guo, Q., and Adhikari, B., 2014. "Understanding the distribution of natural wax in starch–wax films using synchrotron-based FTIR (S-FTIR)." *Carbohydr. Polym., 102*, 125–135.

Nguyen, D.M., Nhung, V.T., Le Do, T.C., Ha-Thuc, C.N., and Perre, P., 2022. "Effective synergistic effect of treatment and modification on spent coffee grounds for sustainable biobased composites." *Waste Biomass Valorization, 13*, 1339–1348.

Qu, Y., Wang, S., Tian, Y., and Zhou, D., 2019. "Comprehensive evaluation of Paraffin-HDPE shape stabilized PCM with hybrid carbon nano-additives." *Appl. Therm. Eng., 163*, 114404.

Robertson, D., van Reenen, A., and Duveskog, H., 2020. "A comprehensive investigation into the structure-property relationship of wax and how it influences the properties of hot melt adhesives." *Int. J. Adhes. Adhes., 99*, 102559.

Sarbu, I., and Sebarchievici, C., 2018. "A comprehensive review of thermal energy storage." *Sustainability, 10*, 191.

Sharma, A., Tyagi, V.V., Chen, C.R., and Buddhi, D., 2009. "Review on thermal energy storage with phase change materials and applications." *Renew. Sustain. Energy Rev., 13*, 318–345.

Tan, Z., Zou, J., Zhang, L., and Huang, Q., 2018. "Morphology, pore size distribution, and nutrient characteristics in biochars under different pyrolysis temperatures and atmospheres." *J. Mater. Cycles Waste Manag., 20*, 1036–1049.

Van Ruijven, B.J., De Cian, E., and Sue Wing, I., 2019. "Amplification of future energy demand growth due to climate change." *Nat. Commun., 10*, 1–12.

Wan, Y., Chen, Y., Cui, Z., Ding, H., Gao, S., Han, Z., and Gao, J., 2019. "A promising form-stable phase change material prepared using cost effective pinecone biochar as the matrix of palmitic acid for thermal energy storage." *Sci. Rep., 9*, 1–10.

Wei, D., Wu, C., Jiang, G., Sheng, X., and Xie, Y., 2021. "Lignin-assisted construction of well-defined 3D graphene aerogel/PEG form-stable phase change composites towards efficient solar thermal energy storage." *Sol. Energy Mater. Sol. Cells, 224*, 111013.

Wu, H., Li, S., Shao, Y., Jin, X., Qi, X., Yang, J., Zhou, Z., and Wang, Y., 2020. "Melamine foam/reduced graphene oxide supported form-stable phase change materials with simultaneous shape memory property and light-to-thermal energy storage capability."

Chem. Eng. J., 379, 122373.

Wu, W., Dai, S., Liu, Z., Dou, Y., Hua, J., Li, M., Wang, Xinyu, and Wang, Xiaoyu, 2018. "Experimental study on the performance of a novel solar water heating system with and without PCM." *Sol. Energy, 171*, 604–612.

Xu, B., and Li, Z., 2013. "Paraffin/diatomite composite phase change material incorporated cement-based composite for thermal energy storage." *Appl. Energy, 105*, 229–237.

Yang, H., Wang, S., Wang, X., Chao, W., Wang, N., Ding, X., Liu, F., Yu, Q., Yang, T., Yang, Z., and others, 2020. "Wood-based composite phase change materials with self-cleaning superhydrophobic surface for thermal energy storage." *Appl. Energy, 261*, 114481.

Yasser, T.M., 2022. Fatty Acid Extraction from Pyrolyzed Spent Coffee Ground Bio-oil (Master Thesis). Tokyo Institute of Technology, Tokyo, Japan.

Yoo, J., Chang, S.J., Wi, S., and Kim, S., 2019. "Spent coffee grounds as supporting materials to produce bio-composite PCM with natural waxes." *Chemosphere, 235*, 626–635.